J Mater Sci: Mater Electron (2016) 27:1427–1432
DOI 10.1007/s10854-015-3907-1

Preparation and characterization of the magnesium aluminate nanoparticles via a green approach and its photocatalyst application

Ruhollah Talebi[1] · Saeid Khademolhoseini[2] · Saman Rahnamaeiyan[3]

Received: 20 July 2015 / Accepted: 16 October 2015 / Published online: 26 October 2015

Abstract Pure magnesium aluminate ($MgAl_2O_4$) nanoparticles were successfully synthesized by novel sol–gel method with the aid of $Mg(NO_3)_2.6H_2O$, $Al(NO_3)_3.9H_2O$, and starch without adding external surfactant. Moreover, starch plays role as capping agent, reducing agent, and natural template in the synthesis $MgAl_2O_4$ nanoparticles. The structural, morphological and optical properties of as obtained products were characterized by techniques such X-ray diffraction, energy dispersive X-ray microanalysis, scanning electron microscopy, and ultraviolet–visible spectroscopy. The sample indicated a ferromagnetic behavior, as evidenced by using vibrating sample magnetometer at room temperature. To evaluate the photocatalyst properties of nanocrystalline magnesium aluminate, the photocatalytic degradation of methyl orange under ultraviolet light irradiation was carried out.

1 Introduction

Nanoparticles have gained much attention among materials, because the nanocrystal properties not only depend on their composition but also depend on their size, shape, and size distribution [1–7]. Global industrialization (such as textile, refineries, leather, paper, chemical, and plastic industries) has used different types of dyes resulted in the release of large amounts of toxic compounds into environment [8]. Generally, 30–40 % of these dyes remain in the waste waters. Additionally, presence of these dyes diminishes the photosynthesis and causes many serious health problems for humanity. To overcome these problems, the waste water from those industries must be treated before their discharge. Various physical and chemical methods have been used for color removal from waste waters. One of these methods is semiconductor photocatalysis and it has proven to be an effective in treating waste water pollution since it is an environmentally friendly, low-cost, and sustainable treatment methodology [9–11]. The search for low cost and efficient photocatalysts is still continuing. Some spinel-type oxides such as $BaCr_2O_4$ [12], $NiFe_2O_4$ [13], $CaBi_2O_4$ [14], $ZnGa_2O_4$ [15], $CuGa_2O_4$ [16], $ZnFe_2O_4$ [17] and $CuAl_2O_4$ [18–20] used as photocatalysts are semiconductor materials with narrow band high and these materials have been proven to be an efficient in the degradation of pollutants and/or the production of photocatalytic hydrogen. Many methods for preparation of nano-sized spinels have been reported such as co-precipitation [21], sol–gel [14–18] sonochemical [16], microemulsion [12] and solution combustion [20]. However, combustion method has many advantages compared to these methods as will be mentioned latter. Additionally, in the combustion technique, nitrates are used as oxidizers, and some organic compounds such as glycine, sucrose, sorbitol, and others are used as fuel. In which the heat released due to the combustion reaction between the oxidizers and the fuel which is exothermic cause can the preparation of the target nanomaterials [21]. Magnesium aluminate spinel ($MgAl_2O_4$) is one of the most famous ceramic material type of metal-oxide with special properties such as high

✉ Saman Rahnamaeiyan
samanrahnamaeiyan@gmail.com

[1] Young Researchers and Elite Club, Central Tehran Branch, Islamic Azad University, Tehran, Iran

[2] Young Researchers and Elite Club, South Tehran Branch, Islamic Azad University, Tehran, Iran

[3] Young Researchers and Elite Club, Borujerd Branch, Islamic Azad University, Borujerd, Iran

melting point (2135 °C), good thermal shock resistance, high mechanical strength, low thermal expansion coefficient, excellent resistance to acid and bases, and also having catalytic and optical properties [22, 23]. Due to these desirable properties, it found widely application in metallurgical, electrochemical, radiotechnical and chemical industries [24]. Thus, the preparation of magnesium aluminate powders with high purity, chemical homogeneity, control of stoichiometry, fine particle size, narrow particle size distribution, and minimum particle agglomeration with high sinter activity has received considerable attention in order to improve the material properties [25]. In many of applications, especially as catalyst support, there has been growing interest to meet the properties such as high surface area, small crystallite size and more active sites in the synthesis of $MgAl_2O_4$ spinel [26]. In recent years, various techniques such as wet chemical techniques and solid-state reaction method have been employed for the production of pure $MgAl_2O_4$ spinel powders. The fabrication of the high purity dense sintering body by conventional solid-state reaction method is often difficult [27] and high temperature calcinations, longer reaction time in this synthesis triggers the grain growth and hard agglomeration [28]. Also inhomogeneity, lack of stoichiometry control, high temperature is the disadvantages of solid-state routes. But various wet chemical techniques have been applied for the synthesis of pure spinel powders at relatively low temperatures to improve the sinterability and fabrication fine particles including hydroxide or carbonate salts co-precipitation, classical sol–gel route, spray drying, freezedrying, mechanochemical synthesis, hydrothermal, microwave-assisted combustion processing, microemulsion and etc. [29–36]. Among the wet chemical routes, Sol–gel technique has been used widely because it has the advantage of producing pure, ultrafine powders at low temperatures, High surface area and pore size distribution. In this report, for the first time, we had presented the preparation of $MgAl_2O_4$ nanoparticles by novel sol–gel method at 800 °C in the presence of starch without adding external surfactant. This approach is simple, low energy consumption and friendly to the environment. A green approach for $MgAl_2O_4$ nanoparticles synthesis by utilizing natural template permits the reaction to proceed usually in milder conditions. Although existing chemical approaches have effectively produced well-defined $MgAl_2O_4$ nanoparticles, these processes are generally costly and include the employ of toxic chemicals. The

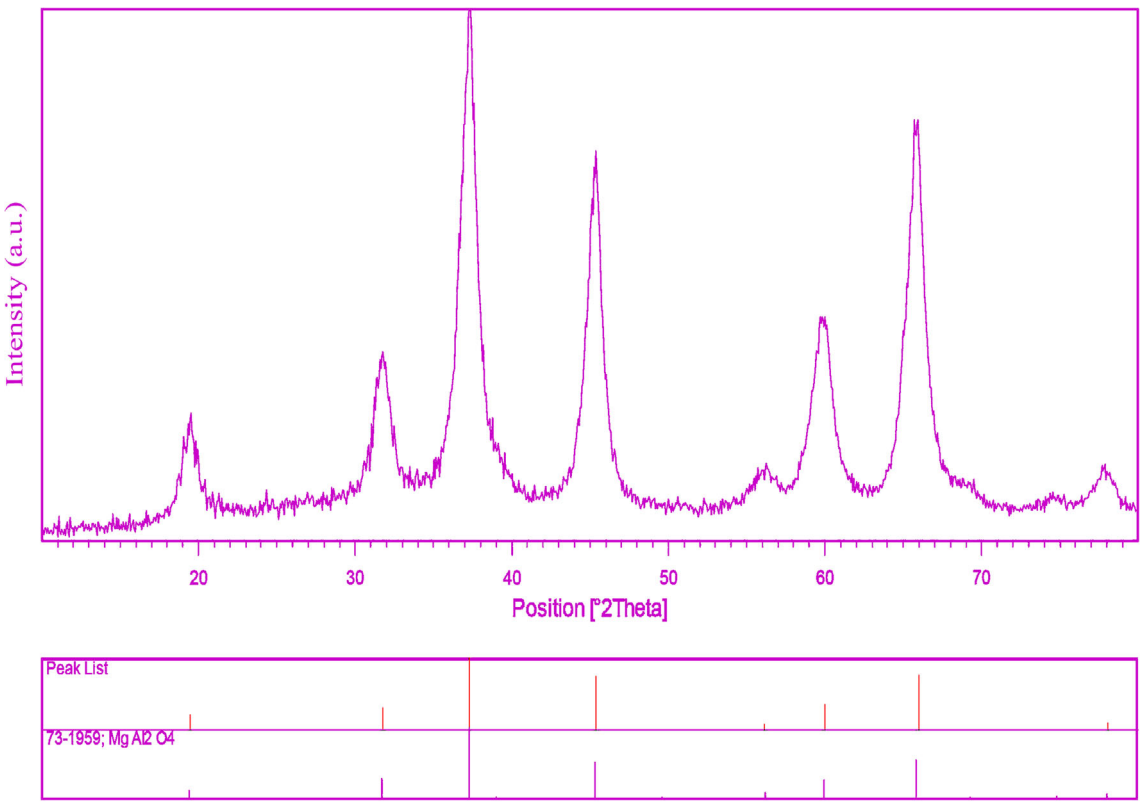

Fig. 1 XRD pattern of $MgAl_2O_4$ nanoparticles calcined at 800 °C

photocatalytic degradation was investigated using methyl orange (MO) under ultraviolet light irradiation [37, 38].

2 Experimental

2.1 Characterization

Magnesium nitrate hexahydrate ($Mg(NO_3)_2{\cdot}6H_2O$), aluminium nitrate nonahydrate ($Al(NO_3)_3{\cdot}9H_2O$), were purchased from Merck Company and used without further purification. X-ray diffraction (XRD) patterns were recorded by a Philips-X'PertPro, X-ray diffractometer using Ni-filtered Cu Kα radiation at scan range of $10 < 2\theta < 80$. Scanning electron microscopy (SEM) images were obtained on LEO-1455VP equipped with an energy dispersive X-ray spectroscopy. The EDS analysis with 20 kV accelerated voltage was done. The magnetic measurement of samples were carried out in a vibrating sample magnetometer (VSM) (Meghnatis Daghigh Kavir Co.; Kashan Kavir; Iran) at room temperature in an applied magnetic field sweeping between ±10,000 Oe. UV–Vis diffuse reflectance spectroscopy analysis (UV–Vis) was carried out using Shimadzu UV–Vis scanning spectrometer.

2.2 Synthesis of $MgAl_2O_4$ nanoparticles

At first, 1.80 g of $Mg(NO_3)_2{\cdot}6H_2O$ was dissolved in 50 mL of distilled water. Then, 6.08 of starch was subsequently added to the above solution under magnetic stirring at 70 °C for 30 min. Afterwards, 5.28 g of $Al(NO_3)_3{\cdot}9H_2O$ was dissolved in 50 mL of distilled water and was added to the above solution under magnetic stirring. A solution was obtained and further heated at 100 °C for 1 h to remove excess water. During continued heating at 110 °C for 1 h, the solution became more and more viscous to become a gel. Finally, the obtained product was calcinated at 800 °C for 2 h in a conventional furnace in air atmosphere and then cooled it to room temperature.

2.3 Photocatalytic experimental

The methyl orange (MO) photodegradation was examined as a model reaction to evaluate the photocatalytic activities of the magnesium aluminate nanoparticles. The photocatalytic experiments were performed under an irradiation ultraviolet light. The photocatalytic activity of nanocrystalline $MgAl_2O_4$ obtained was studied by the degradation of methyl orange solution as a target pollutant. The photocatalytic degradation was performed with 50 mL solution of methyl orange (0.0005 g) containing 0.1 g of $MgAl_2O_4$. This mixture was aerated for 30 min to reach adsorption equilibrium. Later, the mixture was placed inside the photoreactor in which the vessel was 15 cm away from the visible source of 400 W mercury lamps. The photocatalytic test was performed at room temperature. Aliquots of the

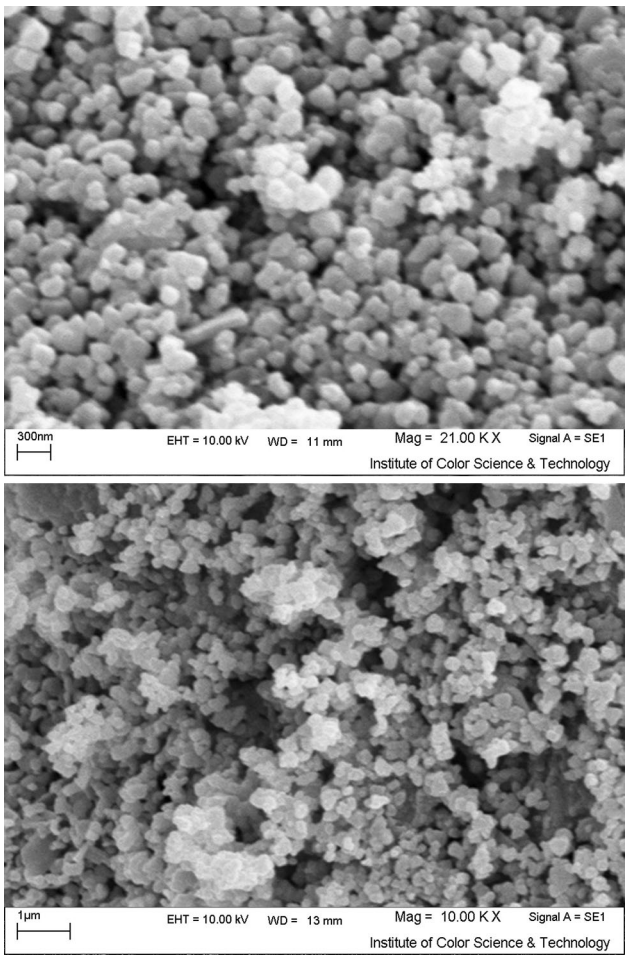

Fig. 2 SEM image of $MgAl_2O_4$ nanoparticles calcined at 800 °C

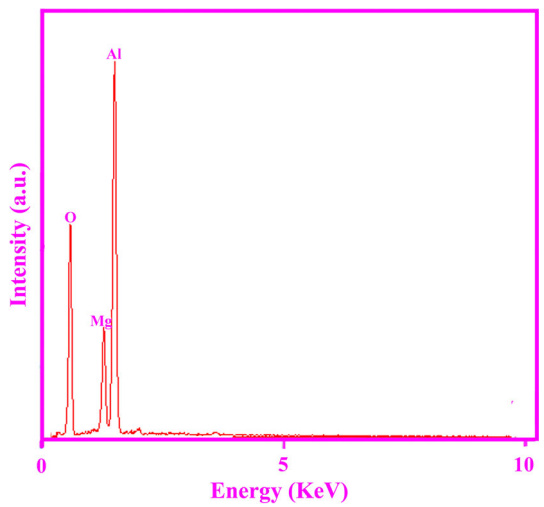

Fig. 3 EDS pattern of $MgAl_2O_4$ nanoparticles calcined at 800 °C

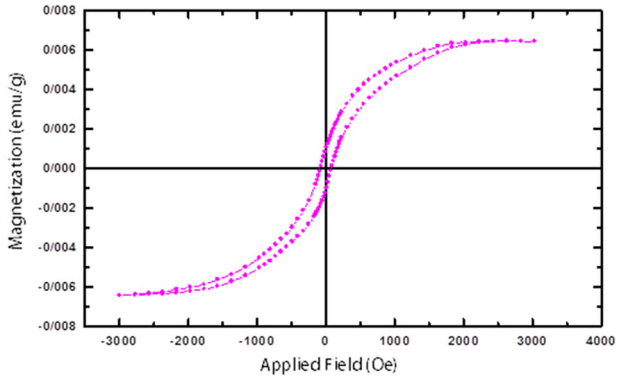

Fig. 4 VSM curve of $MgAl_2O_4$ nanoparticles calcined at 800 °C

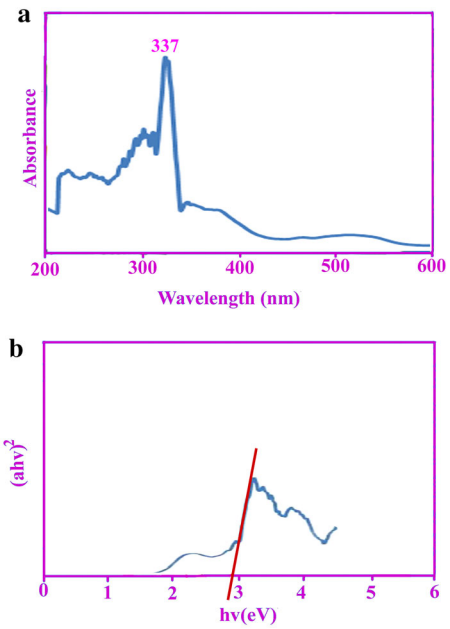

Fig. 5 **a** UV–vis absorption spectra of prepared $MgAl_2O_4$ nanoparticles for 120 min at calcination temperature of 800 °C and **b** plot to determine the direct band gap of $MgAl_2O_4$

mixture were taken at definite interval of times during the irradiation, and after centrifugation they were analyzed by a UV–vis spectrometer. The methyl orange (MO) degradation percentage was calculated as:

$$\text{Degradation rate}\,(\%) = \frac{A_0 - A}{A_0} \times 100$$

where A_0 and A are the absorbance value of solution at A_0 and A min, respectively.

3 Results and discussion

Figure 1 shows a typical XRD pattern ($10° < 2\theta < 80°$) of $MgAl_2O_4$ nanoparticles. Based on the Fig. 1, the diffraction peaks can be indexed to pure cubic phase of $MgAl_2O_4$ (face-centered cubic, Fd–3 m with lattice size of 8.0831°A, JCPDS No. 73-1959). No other crystalline phases were detected. From XRD data, the crystallite diameter (D_c) of $MgAl_2O_4$ nanoparticles was calculated to be 33 nm using the Scherer equation:

$$D_c = K\lambda/\beta\cos\theta$$

where β is the breadth of the observed diffraction line at its half intensity maximum (400), K is the so-called shape factor, which usually takes a value of about 0.9, and λ is the wavelength of X-ray source used in XRD. The morphology of the $MgAl_2O_4$ nanoparticles has been examined by SEM image (Fig. 2). According to the Fig. 2, it is seen

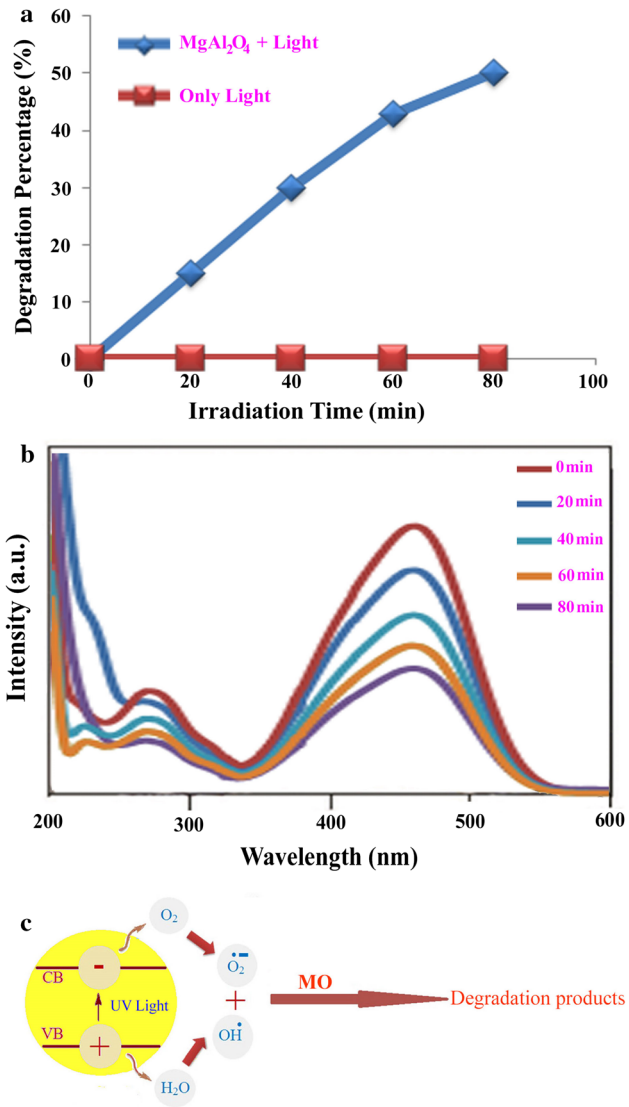

Fig. 6 **a** Photocatalytic methyl orange degradation of $MgAl_2O_4$ nanoparticles under ultraviolet light, **b** fluorescence spectral time scan of methyl orange illuminated at 510 nm with $MgAl_2O_4$ nanoparticles and **c** reaction mechanism of methyl orange photodegradation over $MgAl_2O_4$ nanoparticles under ultraviolet light irradiation

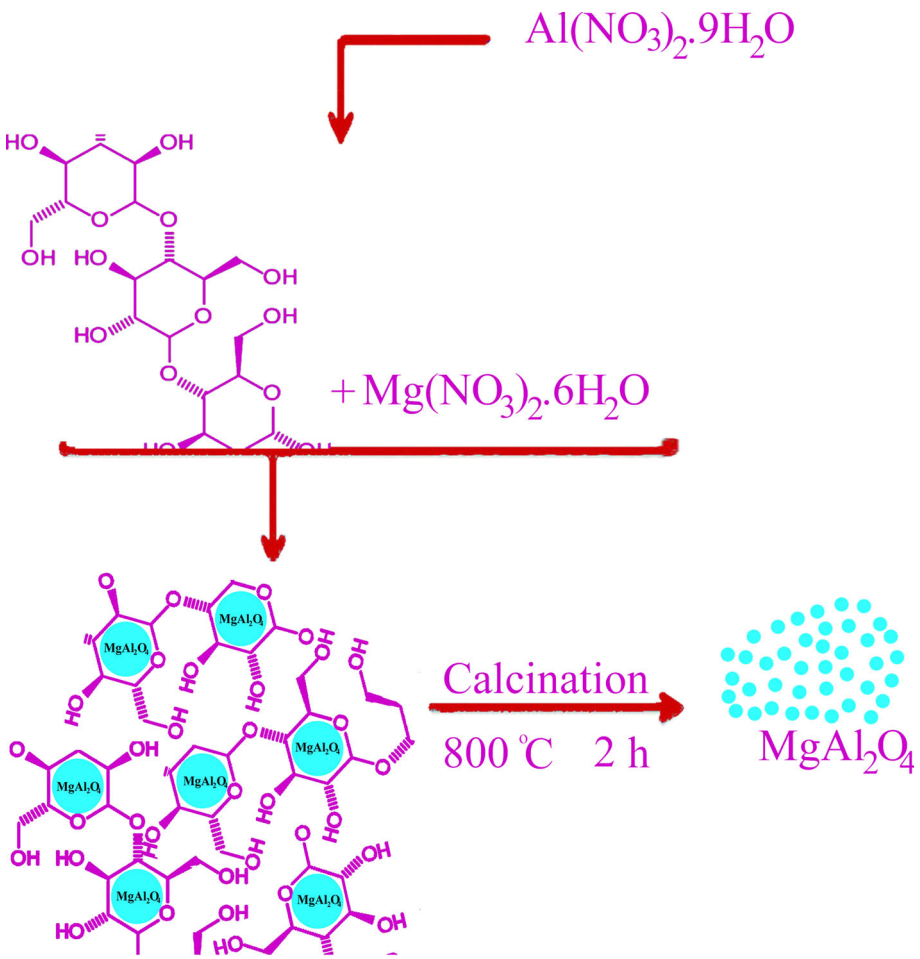

Scheme 1 Schematic diagram illustrating the formation of $MgAl_2O_4$ nanoparticles

that the products composed of small spherical shapes nanoparticles with average size of about 50 nm. The EDS analysis measurement was used to investigate the chemical composition and purity of $MgAl_2O_4$ nanoparticles. According to the Fig. 3, the product consists of Mg, Ti, and O elements. Furthermore, neither N nor C signals were detected in the EDS spectrum, which means the product is pure and free of any capping agent or impurity. The hysteresis loop of $MgAl_2O_4$ nanoparticles was studied to examine their magnetic properties (Fig. 4). At 300 K the remanent magnetization (Mr) is 0.001 emu/g, the coercive field (Hc) is 82 Oe and the magnetization at saturation (Ms) is estimated to be only .006 emu/g (the saturation magnetization Ms was determined from the extrapolation of curve of H/M vs H). The room temperature UV–vis absorption spectra of $MgAl_2O_4$ nanoparticles were also measured in the range of 200–600 nm. Figure 5a shows the diffuse reflection absorption spectra of the $MgAl_2O_4$ nanoparticles calcinled at 800 °C. The figure indicates that the $MgAl_2O_4$ nanoparticles shows absorption maxima at 337 nm, the direct optical band gap estimated from the absorption spectra for the $MgAl_2O_4$ nanoparticles is shown in Fig. 5b. An optical band gap is obtained by plotting $(\alpha h\nu)^2$ versus $h\nu$ where α is the absorption coefficient and $h\nu$ is photon energy. Extrapolation of the linear portion at $(\alpha h\nu)^2 = 0$ gives the band gaps of 2.85 eV for $MgAl_2O_4$ nanoparticles. Photodegradation of methyl orange under UV light irradiation (Fig. 6a–c) was employed to evaluate the photocatalytic activity of the as-synthesized $MgAl_2O_4$. No methyl orange was practically broken down after 80 min without using UV light irradiation or nanocrystalline $MgAl_2O_4$. This observation indicated that the contribution of self-degradation was insignificant. The probable mechanism of the photocatalytic degradation of methyl orange can be summarized as follows:

$$MgAl_2O_4 + h\nu \rightarrow MgAl_2O_4^{\cdot} + e^- + h^+ \quad (1)$$

$$h^+ + H_2O \rightarrow OH^{\cdot} \quad (2)$$

$$e^- + O_2 \rightarrow O_2^{\cdot -} \quad (3)$$

$$OH^{\cdot} + O_2^{\cdot -} + \text{methyl orange} \rightarrow \text{Degradation products} \quad (4)$$

Using photocatalytic calculations by Eq. (1), the methyl orange degradation was about 50 % after 80 min irradiation of UV light, and nanocrystalline $MgAl_2O_4$ presented

high photocatalytic activity (Fig. 6a). The spectrofluorimetric time-scans of methyl orange solution illuminated at 510 nm with nanocrystalline $MgAl_2O_4$ are depicted in Fig. 6b. Figure 6b shows continuous removal of methyl orange on the $MgAl_2O_4$ under UV light irradiation. It is generally accepted that the heterogeneous photocatalytic processes comprise various steps (diffusion, adsorption, reaction, and etc.), and suitable distribution of the pore in the catalyst surface is effective and useful to diffusion of reactants and products, which prefer the photocatalytic reaction. In this investigation, the enhanced photocatalytic activity can be related to appropriate distribution of the pore in the nanocrystalline $MgAl_2O_4$ surface, high hydroxyl amount and high separation rate of charge carriers (Fig. 6c). Furthermore, this route is facile to operate and very suitable for industrial production of $MgAl_2O_4$ nanoparticles. The synthesis pathway of $MgAl_2O_4$ nanoparticles is shown in Scheme 1.

4 Conclusions

In this work, magnesium aluminate nanoparticles were successfully synthesized by a novel sol–gel method at 800 °C for 120 min. The stages of the formation of $MgAl_2O_4$, as well as the characterization of the resulting compounds were done using X-ray diffraction and energy dispersive X-ray spectroscopy. The products were analyzed by scanning electron microscopy (SEM), and ultraviolet–visible (UV–Vis) spectroscopy to be round, about 50 nm in size and Eg = 2.85 eV. VSM analyzes indicates a ferromagnetic behavior for the synthesized nanoparticles. When as-prepared nanocrystalline magnesium aluminate was utilized as photocatalyst, the percentage of methyl orange degradation was about 50 % after 80 min irradiation of UV light.

Acknowledgments Authors are grateful to council of University of Borujerd for providing financial support to undertake this work.

References

1. M. Rahimi-Nasarabadi, J. Nanostruct. **4**, 211 (2014)
2. F. Beshkar, M. Salavati-Niasari, J. Nanostruct. **5**, 17 (2015)
3. M. Ahmadzadeh, M. Almasi-Kashia, A. Ramazani, J. Nanostruct. **5**, 97 (2015)
4. F.S. Ghoreishi, V. Ahmadi, M. Samadpourc, J. Nanostruct. **3**, 453 (2013)
5. A. Rahdar, M. Aliahmad, Y. Azizi, J. Nanostruct. **5**, 145 (2015)
6. E. Khosravifard, M. Salavati-Niasari, M. Dadkhah, G. Sodeifian, J. Nanostruct. **2**, 191 (2010)
7. M. Najafi, H. Haratizadeh, M. Ghezellou, J. Nanostruct. **5**, 129 (2015)
8. J. Safaei-Ghomi, S. Zahedi, M. Javid, M.A. Ghasemzadeh, J. Nanostruct. **5**, 153 (2015)
9. J.S. Piccin, C.S. Gomes, L.A. Feris, M. Gutterres, Chem. Eng. J. **183**, 30 (2012)
10. M.N. Chong, B. Jin, C.W.K. Chow, C. Saint, Water Res. **44**, 2997 (2010)
11. A.A. Firooz, A.R. Mahjoub, A.A. Khodadadi, M. Movahedi, Chem. Eng. J. **165**, 735 (2010)
12. D.F. Wang, Z.G. Zou, J.H. Ye, Chem. Phys. Lett. **373**, 191 (2003)
13. Z.R. Zhu, X.Y. Li, Q.D. Zhao, H. Li, Y. Shen, G.H. Chen, Chem. Eng. J. **165**, 64 (2010)
14. J.W. Tang, Z.G. Zou, J.H. Ye, Angew. Chem. Int. Ed. **43**, 4463 (2004)
15. V.B.R. Boppana, D.J. Doren, R.F. Lobo, Chemsuschem **3**, 814 (2010)
16. K. Gurunathan, J.O. Baeg, S.M. Lee, E. Subramanian, S.J. Moon, K.J. Kong, Int. J. Hydrogen Energ. **33**, 2646 (2008)
17. S.W. Cao, Y.J. Zhu, G.F. Cheng, Y.H. Huang, J. Hazard. Mater. **171**, 431 (2009)
18. Y.Y. Jiang, J.G. Li, X.T. Sui, G.L. Ning, C.Y. Wang, X.M. Gu, J. Sol-Gel. Sci. Technol. **42**, 41 (2007)
19. D.S. Mathew, R.S. Juang, Chem. Eng. J. **129**, 51 (2007)
20. W.Z. Lv, B. Liu, Q. Qiu, F. Wang, Z.K. Luo, P.X. Zhang, S.H. Wei, J. Alloys Compd. **479**, 480 (2009)
21. D. Kovacheva, H. Gadjov, K. Petrov, S. Mandal, M.G. Lazarraga, L. Pascual, J. Mater. Chem. **12**, 1184 (2002)
22. M. Sindel, N.A. Travitzky, N. Claussen, J. Am. Ceram. Soc. **73**, 2615 (1990)
23. H. Zhang, X. Jia, Y. Yan, Z. Liu, D. Yang, Z. Li, Mater. Res. Bull. **39**, 839 (2004)
24. X. Su, X. Du, S. Li, J. Li, J. Nanopart. Res. **12**, 1813 (2010)
25. B. Alinejad, H. Sarpoolaky, A. Beitollahi, A Saberi, S.H. Afshar, Mater. Res. Bull. **43**, 1188 (2008)
26. J.J. Guo, H. Lou, H. Zhao, D. Chai, X. Zheng, Appl. Catalyst A: Gen. **273**, 75 (2004)
27. P.Y. Lee, H. Suematsu, T. Yano, K. Yatsui, J. Nanopart. Res. **8**, 911 (2006)
28. D. Domanski, G. Urretavizcaya, F. Castro, F. Gennari, J. Am. Ceram. Soc. **87**, 2020 (2004)
29. M.M. Rashad, Z.I. Zaki, H. El-Shall, J. Mater. Sci. **44**, 2992 (2009)
30. Z. Haijun, J. Xiaolin, L. Zhanjie, L. Zhenzhen, J. Mater. Lett. **58**, 1625 (2004)
31. X.L. Pan, S.S. Sheng, G.X. Xiong, K.M. Fang, S. Tudyka, N. Stroh, H. Brunner, Coll. Surf. A: Physicochem. Eng. Asp. **179**, 169 (2001)
32. C.T. Wang, L.S. Lin, S.J. Yang, J. Am. Ceram. Soc. **75**, 2240 (1992)
33. K. MacKenzie, J. Temuujin, T. Jadamba, M. Smith, P. Angerer, J. Mater. Sci. **35**, 5529 (2000)
34. X. Zhang, J. Mater. Ch. Ph. **116**, 415 (2009)
35. J. Bai, J. Liu, Ch. Li, G. Li, Q. Du, J. Adv. Pow. Tech. **22**, 72 (2011)
36. F. Meyer, A. Dierstein, Ch. Beck, W. Hrtl, R. Hempelmann, S. Mathur, M. Veith, J. Nanostruct. Mater. **12**, 71 (1999)
37. M. Riazian, J. Nanostruct. **4**, 433 (2014)
38. G. Nabiyouni, D. Ghanbari, S. Karimzadeh, B. Samani Ghalehtaki, J. Nanostruct. **4**, 467 (2014)